This paper first appeared in the eighth print edition of *Photovoltaics International* journal.

Advantages and shortcomings of UMG silicon in photovoltaic device production

Rainer Krause, **Harold Hovel**, **Eric Marshall**, **Gerd Pfeiffer**, **Zhengwen Li**, **Larry Clevenger**, **Kevin Petrarca**, **Davood Shahrjerdi** & **Kevin Prettyman**, IBM Corporation, Yorktown & Fishkill, New York, USA & Mainz, Germany; & **Steve Johnston**, NREL, Golden, Colorado, USA

ABSTRACT

Upgraded metallurgical-grade (UMG) silicon is a lower cost and lower quality form of solar-grade silicon that is capable of producing solar cells at over 16% efficiency. This paper presents some of the economic advantages and technical concerns and solutions associated with producing silicon based PV from UMG, as well as preliminary solar cell results using this material. Results are based on a comparison of cells made in a turnkey line (Schmid Group) using alloy blends of 10%, 20%, 30% and 100% UMG, mixed with solar-grade Si before ingot growth. Detailed characterization was carried out on these finished cells according to lifetime, LBIC, diffusion length and luminescence imaging to determine correlations of performance with basic parameters. Requirements for material cost and cell performance necessary for UMG solar cells to be cost competitive are also presented.

Introduction

Several years ago, the price of silicon-based PV devices was significantly higher (1.5-3.5x, depending on spot vs. locked in prices) than they are today. Due to the plethora of government subsidies in the industry, particularly in Europe, 'high' average selling prices (ASPs) often provided manufacturers with healthy profit margins. However, the amount of subsidies has been decreasing at a significant rate, some to the point of elimination. Additionally, price pressures on silicon-based PV cells and modules from thin-film manufacturers have resulted in costs below US$1/watt.

Roughly half of the cost of a silicon-based cell can be attributed to the cost of raw materials, specifically silicon, which was constrained across the globe due to the large number of new cell producers entering the market, bringing with them a corresponding increased need for the limited silicon. At that point in time, the price of silicon was extremely high, with some spot prices hitting above US$350 per kg for solar-grade material. Longer-term contracts could be locked in at around US$70 per kilogram if the buyer was fortunate.

An alternative then appeared on the scene, one that demanded further technical exploration before it could be used as a silicon source on a large scale in the PV industry. That alternative material was UMG silicon, which, at the time, cost as relatively little as US$30-35 per kg for UMG vs. >US$70 per kg for solar grade. With such a severe price differential, significant cost decreases could be achieved if UMG could provide or could be made to provide the same or nearly the same solar efficiencies and reliability as solar-grade silicon.

Experimental data and findings

The experimental approach used in this review involved the comparison of cells made in a turnkey line using alloy blends of 10%, 20%, 30% and 100% UMG, mixed with solar-grade Si before ingot growth. Measured minority carrier lifetimes ranged from 2 to 8 microseconds in finished cells. Diffusion length maps were not well correlated with lifetime maps on these same cells. A possible explanation is that since the measured diffusion lengths of 200–250 microns (except for the 100% UMG at 140–180 microns) are comparable to the wafer thickness, the measured value may become insensitive

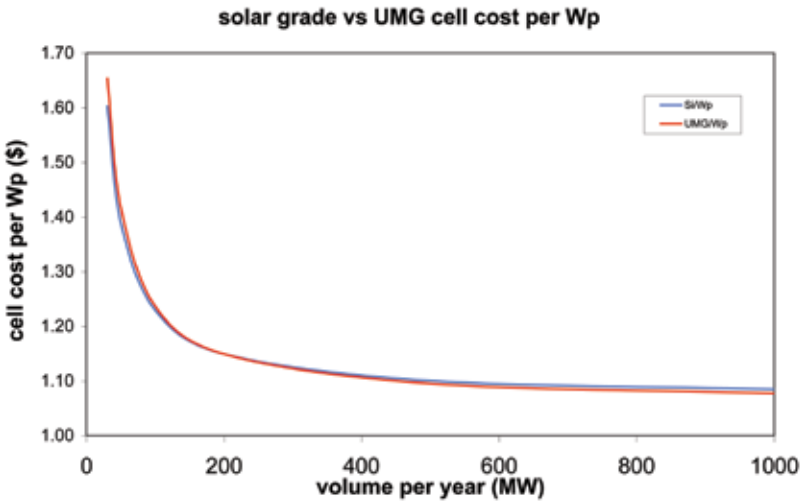

Source: IBM cost model.

Figure 1. Typical learning curve showing cost vs. factory volume. Cell cost is compared per Wp between solargrade and UMG wafer material.

Composition	Resistivity (ohm-cm)	Lifetime (µsec)	Fill Factor (%)	Efficiency (%)
100% UMG	0.5-0.7	1-2	74.1	14.5
30% UMG	1.6-2.7	7-8	73.6	14.6
20% UMG	1.2-3.1	N/A	73.0	14.7
10% UMG	0.7-2.8	N/A	75.2	15.0
Solar Grade	1.8-2.3	8-9	73.2	14.1

Table 1. Comparison of cell parameters for various blends of solar-grade (MEMC) and UMG material.

to the actual value. Similarly, the lifetime values may be adversely influenced by the cell's metallized backside, even though the excitation and detection are both carried out on the wafer fronts. Initial quantum efficiency measurements were also somewhat insensitive to position on the wafer, whether measured in low or higher lifetime regions.

> "With the lifetimes measured after gettering, efficiencies comparable to typical solar grade of >16% are expected for UMG-based material."

Forensic loss analysis is being used to ascertain major contributors and detractors to device performance. Optical losses in the blue-coloured surfaces amount to between 8 and 9%. All solar cell parameters were lower than normal: V_{oc} values are 610–620 millivolts, with photocurrents of 31 to 33mA/cm^2 and FF values of 0.72 to 0.75. High shunt conductances may account for the low fill factors and V_{oc}s, while slightly high series resistances may account for lower short circuit currents. However, the low photocurrent values are consistent with the measured lifetimes and diffusion lengths. Solar cell modelling was used to investigate the reasons for the lower performance, which was mostly due to the poor lifetime values.

Phosphorus gettering at 840 to 900°C for 30 to 90 minutes raised the starting effective lifetime to as much as 110 microseconds in the 20% UMG blend (20% UMG/80% solar grade) and 70 to 80 microseconds in all other blends. The 100% UMG was the exception, where lifetimes of only 20 microseconds were obtained. Lifetime maps show that larger grain size regions exhibited the largest lifetime improvement while small grain regions closer to the wafer edge showed the least improvement. Lifetimes of 10–20 microseconds are consistent with the diffusion lengths of 200–250 microns observed. A lifetime of 20 microseconds in the 100% UMG material after gettering would have boosted the diffusion length in that material by a factor of two, raising the efficiencies to the 15% observed in the UMG/solar-grade blends. With the lifetimes measured after gettering, efficiencies comparable to typical solar grade of >16% are expected for UMG-based material.

Economics and justification for investigating UMG

There are a number of UMG producers in the market providing a product that potentially could produce a cost advantage over competitors, inside and outside of the silicon-based PV industry. It is necessary for UMG to have acceptable (equivalent?) efficiency and reliability, comparable to devices made from semiconductor or solar-grade material, which had been in use for nearly 30 years. One such producer of this material is New York-based Globe Specialty Metals (GSM).

Efficiency is a relatively simple and quick measurement to make and a producer's claims can be easily verified. Reliability measurements are not quite so simple, however. Claims are often made in the industry regarding a product's longevity with very little data available to back them up. Since there are so many relatively new companies producing PV devices, very few have cells that have been operating for the 20 to 30 years often expressed in the warranty. Relatively little work has been done in acceleration studies often used in the semiconductor industry in order to determine the Weibull plots and parameters needed to predict failure within a population. Temperature and humidity chambers needed for the studies exist, but the mathematical relationship between the various parameters are often not well understood.

If one could show that UMG is or can be made less expensive with an efficiency on par with solar-grade material, and have an acceptable reliability, then the 'holy grail of grid parity targets often discussed by those in the industry would be closer to being achieved in multiple geographies.

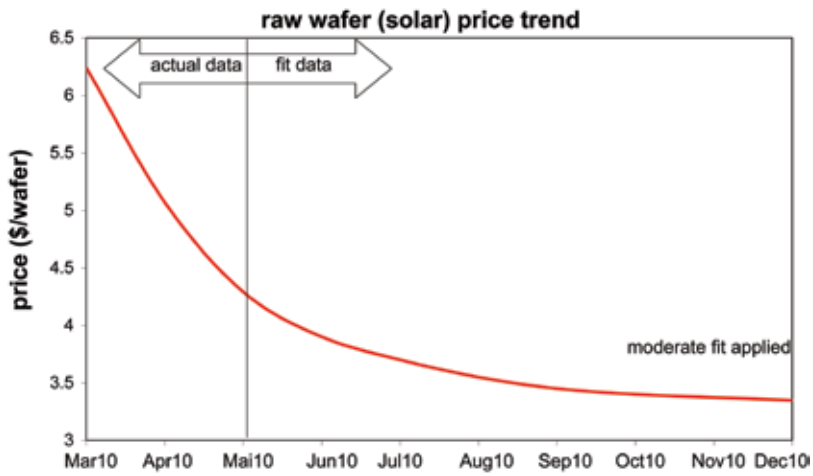

Source: BDEW, pvXchange & solarserver.

Figure 2. Solar-grade wafer cost data and future projection for 2010.

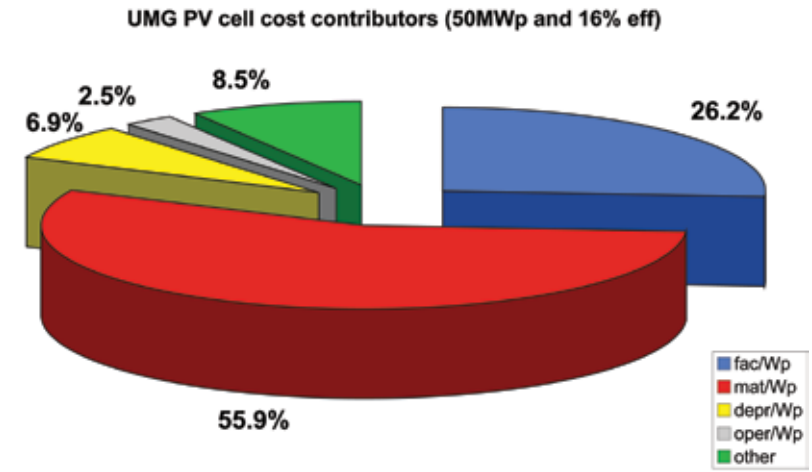

Source: IBM cost model

Figure 3. Cell cost contributors for silicon and UMG wafers.

	solar grade 16% eff.	UMG 16% eff	UMG 15.5% eff	UMG 15% eff	UMG 14.5% eff	UMG 14% eff
$ cost/wafer	3.3	3.1	3	2.9	2.8	2.7
Wp/cell	3.89	3.89	3.77	3.65	3.53	3.41
Δ UMG/Si	0%	6.1%	9.1%	12.1%	15.1%	18.1%

Table 2. UMG data for solar-grade matching cost conditions.

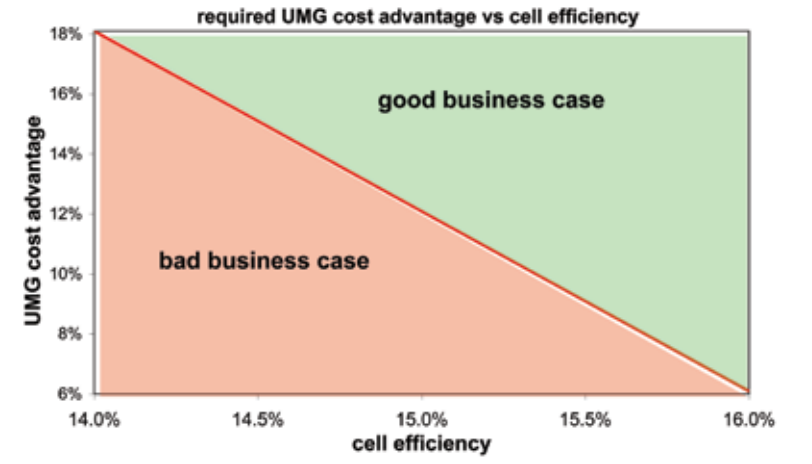

Source: IBM cost model

Figure 4. Break-even cost advantage needed for lower solar efficiencies in UMG cells, assuming gettering processes and equipment are included in a manufacturing line.

Cost

Cost estimation and comparison between cells made from UMG and cells made from solar-grade material were performed for this study. Although our initial investigation showed roughly equivalent measured parameters between UMG (ungettered) and solar-grade cells (see Table 1), a worst-case scenario is assumed in this analysis, where gettering is considered necessary to achieve equivalency. In Table 1, efficiency was relatively low for all compositions since all cells were made in a non-optimized lab. The importance of the data is shown in the insignificant delta between the various blends, indicating that UMG has a potential path forward, especially if process and material enhancements already known for solar grade are also applied to UMG.

If the worst-case scenario is assumed for this economic analysis, a UMG line would require additional equipment which has to be considered in the cost estimate. The additional capital investments include a phosphorus diffusion furnace as well as a chemical etch bath. The diffusion furnace can be in-line if only relatively short diffusion times are needed, or off-line if diffusion is done before cell production begins. This off-line diffusion operation could be done at the cell producer's facility or at the wafer provider's facility before delivery. This particular diffusion is a phosphorous getter in which impurities are pulled to the surface of the wafer [2] and then 5-20μm (less if after saw damage etch; more if before saw damage etch) is etched off to remove the high impurity layer. With these two additional processes, the entire lead time could be extended by around 1.5 hours. Fig. 1 shows a cost comparison for solar grade vs. UMG at year end 2010, taking into account the lower cost UMG wafer's needs for additional process time and equipment. The following assumptions were made for the cost comparison:

- Manufacturing yield: 95%
- Line utilization: 90%
- Solar-grade Si wafer cost: US$3.3
- UMG wafer cost: US$3.1
- Base efficiency assumption for solar-grade material: 16%
- Base efficiency assumption for gettered UMG: 16%

Although not immediately apparent from the graph in Fig. 1, when UMG material is ~7% less expensive than a solar-grade wafer, overall cell cost is shown to be equivalent. A UMG wafer with an even larger cost differential to solar grade would present a positive business case for using UMG. Solar-grade wafer price data used to perform this cost estimation are shown in Fig. 2.

If this simulated curve is not followed and solar-grade material price does not

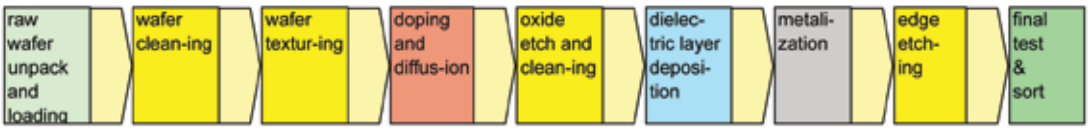

Figure 5. Typical Si turnkey manufacturing flow.

Figure 6. UMG turnkey manufacturing flow.

decline as rapidly as shown, reaching US$3.3 per wafer by end of year, then an even better business case exists for running a line with UMG rather than solar-grade material. The estimated numbers for end of year 2010 used the US$3.3 per wafer cost. Current (April 2010) wafer cost is US$5.07 US with May's cost estimated to be at or near US$4.29. The graphs in Fig. 3 show the cell costs broken down by contribution.

The pie charts show, as discussed previously, that in the case of UMG the material cost is reduced but depreciation and facility-related costs are higher. The lower material cost must at least compensate for the higher depreciation and facilities costs.

If the assumption is made that UMG-based cells have a lower solar efficiency than solar grade even with the gettering process implemented, the cost advantages have to be even better, as shown in Table 2. The solar-grade reference assumes a 16% solar efficiency. This data is presented graphically in Fig. 4.

This figure shows that UMG material operating at 14% efficiency needs at least an 18% material cost advantage in order to compete with solar-grade material operating at 16% efficiency.

Characteristics of UMG and comparison with solar-grade material

Polysilicon feedstock used to produce solar-grade multicrystalline wafers has traditionally relied on scrap material from semiconductor wafer production or semiconductor-grade 'poly' produced directly for this purpose. Semiconductor-grade Si is obtained by processing metallurgical-grade Si through the Siemens process where impurities are removed chemically by conversion to chlorosilane compounds with multiple distillations. While the Siemens process is effective in removing impurities down to the ppb level (10^{13}cm^{-3}), its energy budget at approx. 200kWh/kg is substantial, which in turn drives high costs for the finished product.

An attractive route to reducing material costs in PV applications is to avoid the Siemens process and purify metallurgical-grade (MG) Si using alternative processes. This has to be done at lower cost and improved energy efficiency while still reducing impurities to levels of 1 ppm (10^{16}cm^{-3}) and below, a level that is necessary for building solar cells at efficiencies similar to standard solar-grade material. Critical impurities are boron (B) and phosphorous (P) in terms of dopant level control and carbon (C), oxygen (O), iron (Fe), titanium (Ti) and calcium (Ca).

Element	B(Wet)	Na	P(OES)	Ca	Ti	V
ICP-MS (PPBw)	586.345	737.70	2,230.0	2,159.12	49.424	19.307
Element	Cr	Mn	Fe	Ni	Cu	Zn
InCP-MS (PPBw)	24.39	0.042	2,403.47	25.266	33.67	998.44
Element	As	Se	Rb	Sr	Zr	Nb
ICP-MS (PPBw)	0.130	0.023	14.556	78.485	163.76	1.958
Element	Mo	Ru	Cd	Sb	La	Ce
InCP-MS (PPBw)	3.556	4.779	0.021	8.508	0.229	1.395
Element	Pr	Nd	Sm	Gd	Tb	Dy
InCP-MS (PPBw)	0.339	0.131	0.007	0.029	0.002	0.055
Element	Er	Tm	Ta	Re	Pb	U
InCP-MS (PPBw)	0.084	0.055	3.615	0.01	0.034	0.177

Table 3. Elemental analysis UMG material from Solsil Corp.

To purify MG Si, a number of strategies [3] have been developed to extract impurities from liquid molten Si, producing upgraded MG (UMG) Si. The actual impurity level of MG Si to be refined depends on the purity of the quartz raw material and the reduction process used. The UMG process may have to be adjusted to the specific properties of the MG used. All UMG is not equivalent, and it is assumed to have had unexpected results for more than one manufacturer of solar cells. Impurity levels in the low ppm range and below are shown in Table 3. UMG feedstock is used in a standard casting and wafering process to produce multicrystalline wafers for use in PV manufacturing. Several cell manufacturers are now in high-volume production using UMG-based wafers.

For comparison, we show impurity levels measured on a commercial solar-grade wafer in Table 4, where it is apparent that the solar-grade sample contains significantly higher concentrations of Cu whereas Fe is higher in this particular UMG. Ni is in the same range for both materials. These elements are expected to be key contributors to carrier lifetime degradation due to charge carrier recombination.

One avenue to further improve the properties of UMG material is by blending it with solar-grade material, which has been demonstrated recently by blending the two materials at the ingot casting step [1]. As discussed, this approach holds promise for accelerating the adoption of UMG Si in PV manufacturing.

Manufacturing with UMG

The use of a regular turnkey manufacturing line requires solar-grade wafer material to manufacture solar cells. A typical Si turnkey process flow is shown in Fig.5.

Element	Concentration (PPBw)
Al	39
Fe	394
Ni	42
Cu	2630

Table 4. Contamination SIMS analysis of a commercial solar-grade wafer performed by IBM.

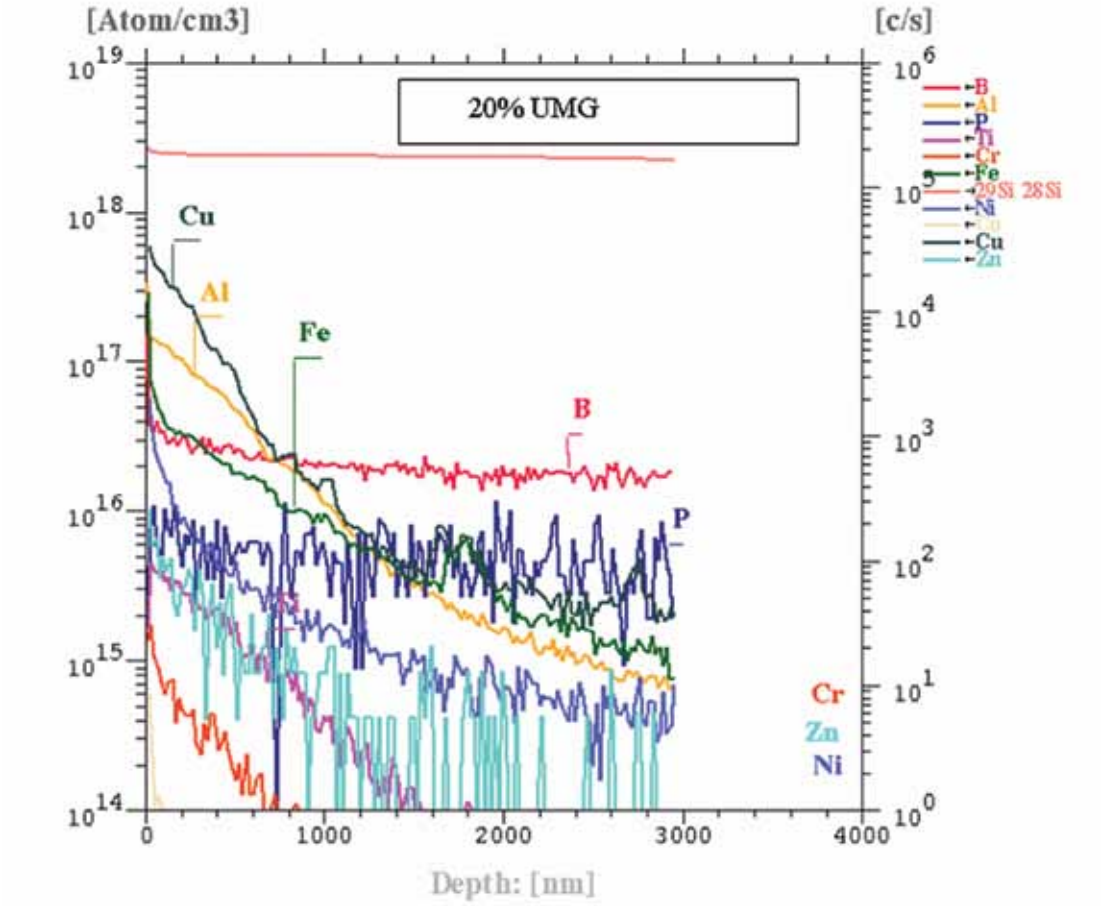

Source: IBM cost model

Figure 7. SIMS profile of 20% UMG starting material.

The typical turnkey line is capable of manufacturing cells with an average efficiency level of around 16%. The yields are typically at 95% with line utilization of around 90%. A turnkey line that can handle UMG material could require some enhancements to prepare the UMG wafers for further processing. Here, we assume that the gettering previously discussed is incorporated in-line in order to reduce the metallic content within the UMG material. A possible line layout is shown in Fig. 6.

In this case, the gettering is applied after the first cleaning step. The additional process steps have an impact on lead time. The doping and diffusion could be performed using $POCl_3$ or H_3PO_4 technology to apply phosphorous doping, resulting in a lead time of at least one hour to achieve a doping depth of ~1µm. The subsequent PSG glass removal by HF etching would then be used before KOH etching of the gettered, high impurity material, at which point the wafers would continue in the normal cell processing sequence.

The additional process steps in the UMG manufacturing flow could add about 1.2 hours to the cell process time and, again, would require additional investments into phosphorus furnace and etch bath equipment.

UMG casting and manufacture of starting material

When producing multicrystalline Si wafers for PV, solar-grade or UMG material is melted in a specialized furnace and then, through a process of controlled solidification termed 'casting', an ingot is prepared. The ingot is cut to dimensions appropriate for the desired wafer cross-section (for example, 156mm x 156mm) and individual wafers are then cut from the block or brick by wire saw in the wafering process. Ingot casting is a critical step in the process where key parameters of the mc material structure and electronic properties are defined. There are a number of different approaches to casting technology including controlled directional solidification, electromagnetic casting and the heat exchange method.

"Materials prepared by different methods typically show differences in some of the relevant properties."

Materials prepared by different methods typically show differences in

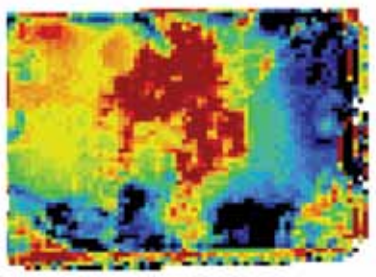

Figure 8. Minority carrier lifetime map of 20% UMG starting material.

Material	B	P	Fe	Ti	Cu	Ni	Zn	Cr	Al
S.G.	1.8E16	1E15	9E14	9E14	1E16	3E14	7E14	1E14	3E15
10%	2E16	1E15	2E15	<1E15	1E15	2E14	5E14	1E14	5E14
20%	2.5E16	5E15	3E15	<1E14	1E15	5E14	1E14	<1E14	1E15
30%	3.5E16	2E16	1E15	<1E14	2E15	3E14	1E14	<1E14	5E14
100%	1.5E17	5E16	7E15	3E14	6E16	4E14	3E14	<1E14	3E15

Table 5. Impurity densities in various UMG/solar-grade blends.

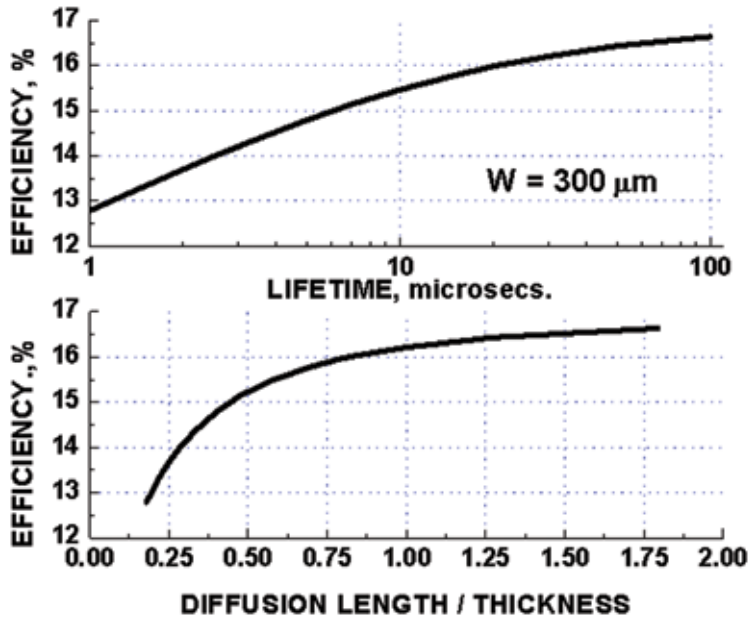

Figure 9. Simulated effect of minority carrier lifetime on efficiency (top), and the effect of the diffusion length to thickness ratio (bottom). (No selective emitter, no back surface field other than Al alloying used.)

some of the relevant properties such as crystallite grain size and distribution, grain boundary structure and defects, dislocation density within the grains and concentration of C, N and O as well as residual metal impurities (for example, Fe, Cu, Ti). Sources of impurities are the feedstock starting material and the furnace and heater surfaces (typically Si_3N_4 and graphite) which come in contact with Si material at high temperature. Impurity segregation during the crystallization process leads to inhomogeneous impurity concentration profiles along the length of the ingot, which in turn leads to variation in cell efficiency of wafers cut from different positions within the same ingot. By managing segregation, ingot sections can be produced with impurity levels lower than the starting feedstock while concentrating impurities at the end portions, which are usually not usable.

From a cost perspective, it is obviously important to maximize the portion of usable ingot, and industry data show that yields in the range from 70-90% have been achieved. During the crystallization process, precipitates of SiO_2, Si_3N_4 and SiC can be formed in the melt and the ingot. While SiO_2 precipitates are useful in terms of being able to getter metallic impurities, Si_3N_4 and SiC are assumed to degrade cell efficiency [4]. Metal decoration of intergranular defects plays a major role in limiting carrier lifetime. This means that for UMG material, the control of metal-related defects during the casting process is critical to improving efficiency.

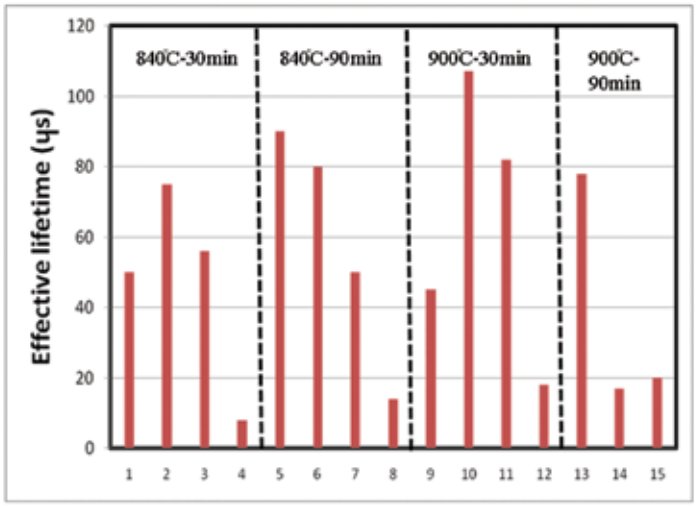

SolarGrade	1	5	9	13
UMG20	2	6	10	-
UMG30	3	7	11	14
UMG100	4	8	12	15

Figure 10. Phosphorus gettering results for solar grade and for several UMG blends.

Characterization of starting material and devices

In order to optimize the lower cost benefits of UMG material, solar cells made from this material should be at least comparable in efficiency to devices made from the higher cost solar-grade starting wafers. As with any solar cell fabrication, characterization of the starting wafers can allow removal of the poor quality material before any value-added device processing takes place. The most important pre-process characterization of the starting material is an evaluation of the minority carrier lifetime, assuming there are no critical cracks, indentations, broken corners, or other physical failure mechanisms existing in the wafer. The lifetime depends on impurity content, grain boundaries, dislocation networks, and other types of defects. Relative oxygen content will also play a role, especially in subsequent light-induced degradation associated with boron and iron content [4].

Table 5 shows impurity content of selected elements as measured by SIMS for the various composition blends used in this study ranging from solar-grade material (S.G.) to 100% UMG. Fig. 7 shows a SIMS plot for 20% UMG material. The total heavy metal population is around low $10^{16}cm^{-3}$, similar to the boron dopant concentration. The exception is the 100% UMG material, which exhibits impurity densities 5-10x higher than the other blends for boron, iron and copper. All the blends of solar grade and UMG were p-type with resistivities of roughly 0.5–1Ω/cm. Impurity levels appeared much higher at the surface compared to the bulk, but it is possible that this measurement is influenced by surface roughness.

The oxygen is usually in the low $10^{17}cm^{-3}$ range in solar-grade materials and likely to be comparable in the UMG/solar-grade

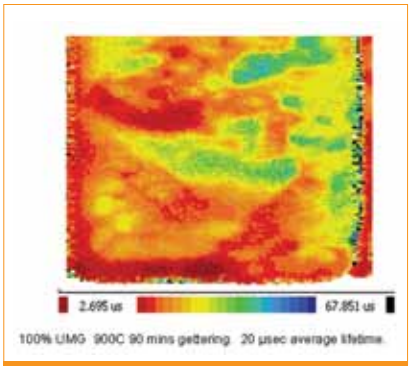

Figure 11. Lifetime map of gettered 100% UMG starting material after 90 minutes phosphorous diffusion.

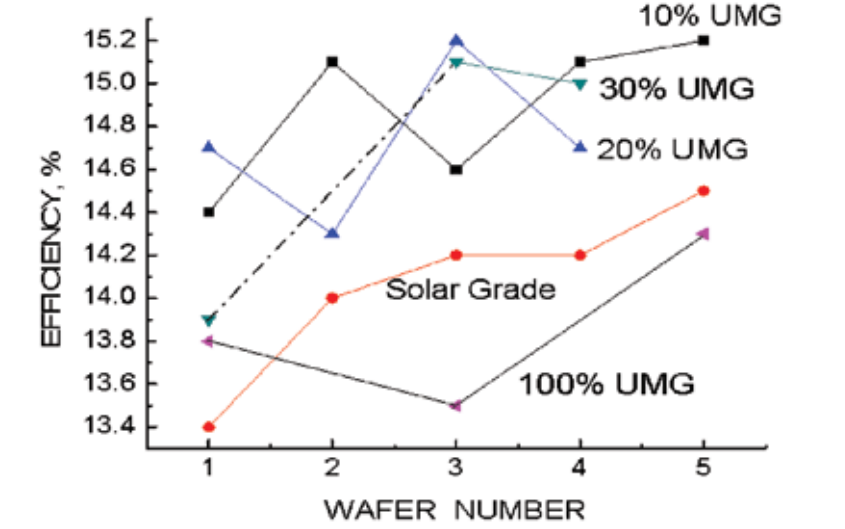

Figure 12. Efficiencies of cells made from the different UMG blends.

blends, although results were inconclusive when those measurements were made. Further investigation is merited in this case.

As mentioned earlier, the minority carrier lifetime plays a crucial role in the performance of the devices. This manifests itself in calculations of efficiency versus lifetime and/or efficiency versus the diffusion length/wafer thickness ratio. As the wafers become thinner, light trapping becomes increasingly essential. An acceptable degree of light trapping for wafers several hundred microns thick or below is typically provided by texturing, causing light entering the Si to travel at oblique angles.

For UMG blends, the starting lifetime can be relatively low before impurity gettering. Efficiency is a strong function of lifetime. A lifetime map of 20% UMG starting material using microwave photoconductivity decay (μPCD) is shown in Fig. 8. Lifetimes of 1 to 1.5 microseconds are typical of the UMG material and also of some solar-grade material as received from wafer vendors. Pockets of lower and higher lifetime are observed in these maps, possibly associated with dislocation networks at smaller grain boundary intersections.

Even small improvements in lifetime can dramatically improve the device performance. If the lifetime is improved sufficiently for the diffusion length to exceed the wafer thickness, the performance becomes both higher and less sensitive to changes in lifetime. These observations are shown in Fig. 9, which shows efficiency versus thickness and efficiency versus the diffusion length/wafer thickness ratio for a range of lifetime values as they would exist in finished devices. Improving the starting lifetime from a typical value of 1-2 microseconds up to 10-20 microseconds or higher has a substantial benefit. Simulations depicted in Fig. 9 do not include the benefits of a local back-surface field or a double emitter, which could potentially enhance the device performance by as much as several percent.

> "As the wafers become thinner, light trapping becomes increasingly essential."

As discussed, lifetime can be improved significantly by gettering. Experiments were carried out to determine what improvements could be obtained for the various UMG blends as a function of anneal conditions. Gettering was carried out by $POCl_3$ diffusion between 840 and 900°C for 30 to 90 minutes. Prior to gettering, the wafers were saw damage etched and cleaned with CP4 ($HF:HNO_3$: acetic acid) and RCA etch ($HCl:H_2O_2:H_2O$) before loading into the $POCl_3$ furnace. After the anneal, the phosphor silicate glass (PSG) oxide was etched off and the samples were measured with iodine passivation.

Type	<J_{sc}>	<V_{oc}>	<FF>	<J_{01}>	<J_{02}>	<R_{SH}>	R_{SER}	Effic.
Sol. Grade	32.1	.590	.744	2.65^{-12}	1.08^{-7}	3110	0.79	14.1
10% UMG	32.3	.6064	.760	1.52^{-12}	6.79^{-8}	4490	0.695	14.9
20% UMG	31.9	.6044	.763	1.70^{-12}	6.03^{-8}	3780	0.667	14.7
30% UMG	32.1	.6027	.760	1.72^{-12}	8.10^{-8}	5030	0.695	14.7
100% UMG	30.3	.621	.740	5.51^{-13}	9.38^{-8}	4750	0.631	14

Table 6. Solar cell parameters from UMG blends using process 3.

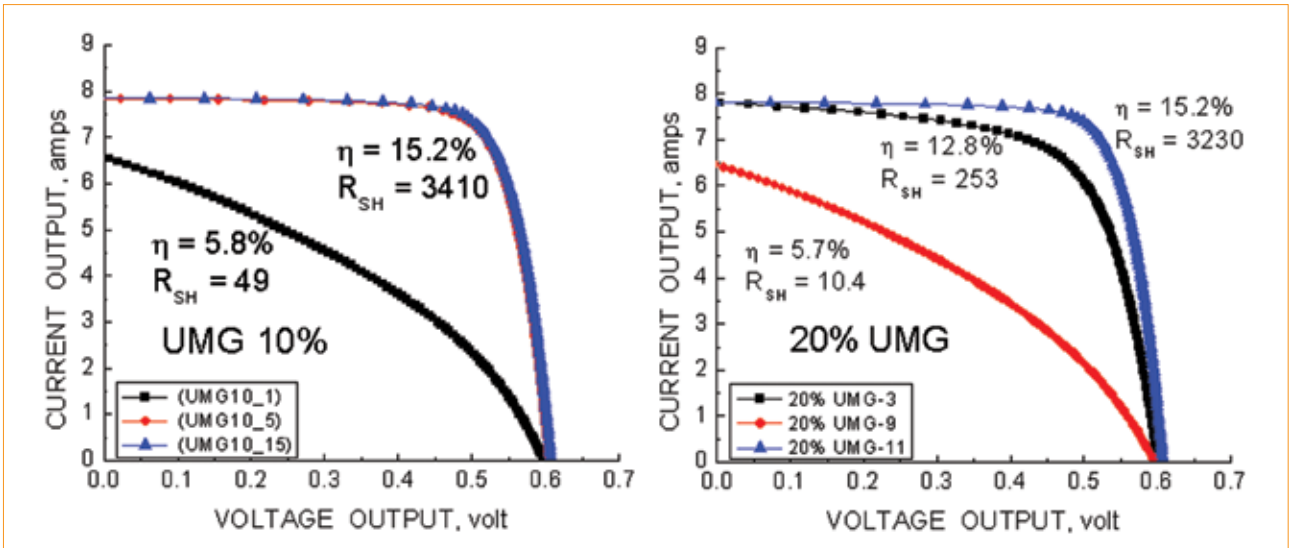

Figure 13. Current-voltage behaviour under 1 sun illumination for 10% and 20% UMG cells.

Fig. 10 shows the lifetime results for UMG blends 0%, 20% 30%, and 100% UMG, and Fig. 11 shows a lifetime map measured by µPCD on the 100% UMG material. Gettering had a dramatic effect on improving the lifetime, which increased to 50 to 80 microseconds for the 20% and 30% blends, respectively, even exceeding 100 microseconds at one point. All the UMG blends performed well but 100% UMG was not as receptive to the gettering as the others. From Table 3, the 100% UMG is shown to have from 5 to 10x more impurities than the other blends, so a lower response to the gettering of these impurities would be expected. More extensive gettering is probably needed.

> "The implication is that UMG feedstock could be mixed with solar grade to obtain equivalent device performance at somewhat lower cost."

If lifetimes greater than 20 µsecs can be obtained in 100% UMG, efficiencies exceeding 16% are obtainable, comparable to present-day multicrystalline cell efficiencies as obtained in turnkey fabrication lines. Advanced device designs, which include selective emitters and improvements in back-surface fields, would be expected to increase the efficiencies to higher values in UMG just as in solar-grade material.

Characterization of finished devices

Wafers from 10%, 20%, 30% and 100% UMG blends and solar-grade controls were processed in the solar cell fabrication turnkey line at Schmid GmbH using H_3PO_4 mist as the diffusion source, along with PECVD SiN passivation/AR coating on the acid-textured surface and screen-printed Ag (front) and Al (back) contacts. The wafers were 156 x 156mm squares but only 15 wafers of each blend were available. These were divided into three process sequences: 1) standard emitter diffusion to 50Ω/⊗; 2) double-sided phosphorus diffusion also with 50Ω/⊗ and the rear side diffusion etched off; 3) one-hour phosphorous diffusion at 865°C. N^+ layers were removed from both sides, and the wafers continued as in process 1 (see [1] for further details).

The efficiencies, I-V behaviour, spectral response, and diode properties of the wafers were measured both at Schmid and at IBM. Lifetime, diffusion length, LBIC (light beam-induced current) and reflectance maps were made using a µPCD – LBIC mapper (Semilab Corporation). Photo and electroluminescence, and DLIT (dark lock-in thermography) maps were made at NREL.

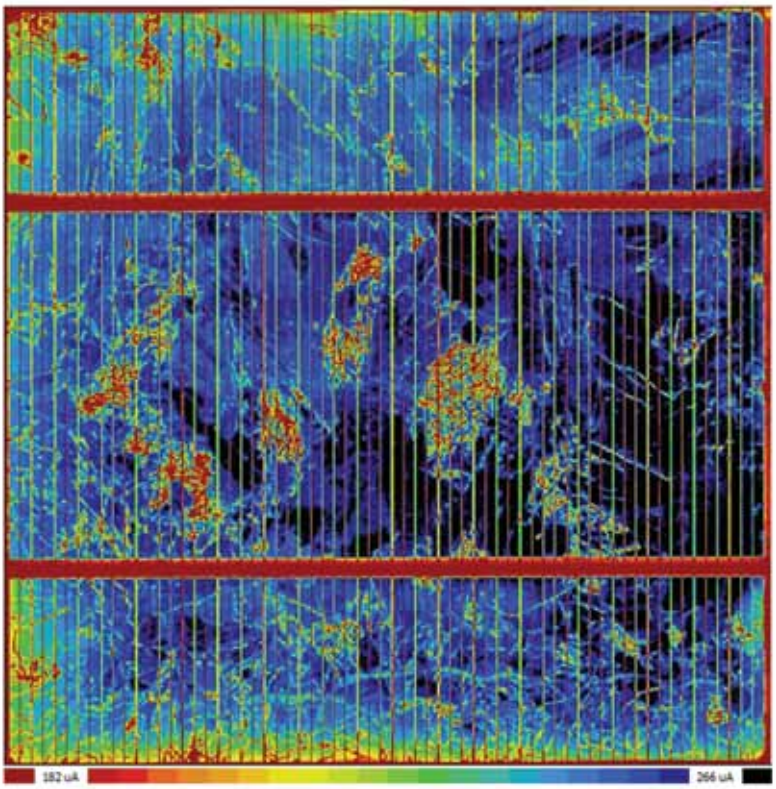

Figure 14. LBIC map of a shunted 10% UMG cell showing patches of higher dislocation density.

Table 6 shows average device parameters for the four blends and solar grade using process 3 in each case, so some degree of gettering was present. The lifetimes in the finished wafers were around 8 microseconds [1]. Electrical parameters from all the materials are nearly the same except for the 100% UMG, which exhibited lower photocurrents due to poorer lifetimes and higher V_{oc}, most

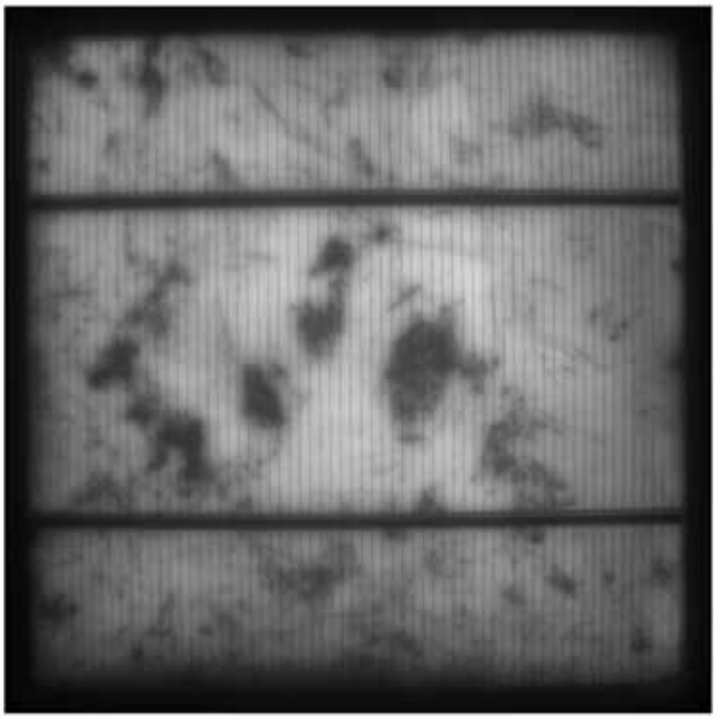

Figure 15. Photoluminescence map of the shunted cell shown in Fig. 8, indicating exact correspondence with regions of lower photocurrent (= lower lifetime).

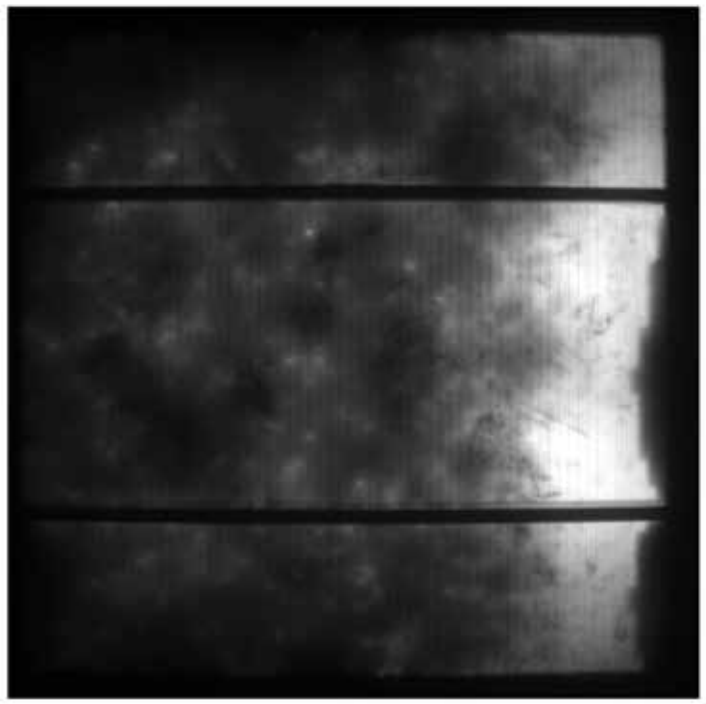

Figure 16. Forward bias electroluminescence map of the shunted cell in Figs. 8 and 9. Dark areas are regions of low lifetime and low current.

likely due to lower bulk wafer resistivity. Fill factors, J_{01} and J_{02}, and series and shunt resistances were all very similar. The implication is that UMG feedstock could be mixed with solar grade to obtain equivalent device performance at somewhat lower cost. Fig. 12 shows the efficiencies at 1 sun intensity for the five types of material and again shows near equivalence except for the 100% UMG. Since the 100% UMG wafers started out with much higher impurity densities, a greater degree of gettering would likely be beneficial for this material compared to the others.

The largest limitation to cell efficiency appears to be shunt conductance. Shunts represent leakage currents through the device which reduce the fill factor and can reduce the V_{oc} in severe cases. Fig. 13 shows I-V curves under 1 sun illumination for 10% and 20% UMG devices. The curves were picked to represent good, medium, and poor shunt resistance cells, illustrating the drop in efficiency with increased leakage current. There was a strong variation in shunt leakage between cells of all UMG blends as well as the solar-grade control. However, the series resistances did not vary significantly between UMG blends or different cells within a particular UMG blend.

"The shunts themselves appear to arise when the bus bars and/or fingers cross high dislocation density patches."

To better understand the possible causes of shunt resistances as well as non-uniformities on the finished cells, maps of LBIC, luminescence, and DLIT were made on all of the cells and a consistent pattern was observed. Fig. 14 shows an LBIC map of a shunted 10% UMG cell where the lifetime varies by a factor of about 2 over the wafer. There are many red/orange-coloured patches at various positions which may represent areas of higher dislocation density. Similar patches to these were observed in nearly all wafers.

Fig. 15 shows a photoluminescence image of the same wafer as that shown in Fig. 14. In images such as these, bright areas usually represent higher lifetimes and darker areas represent lower lifetimes, localized areas where recombination centres are present in higher density. This is more likely to occur in high dislocation density areas. Comparison of Figs. 14 and 15 show a one-to-one correspondence

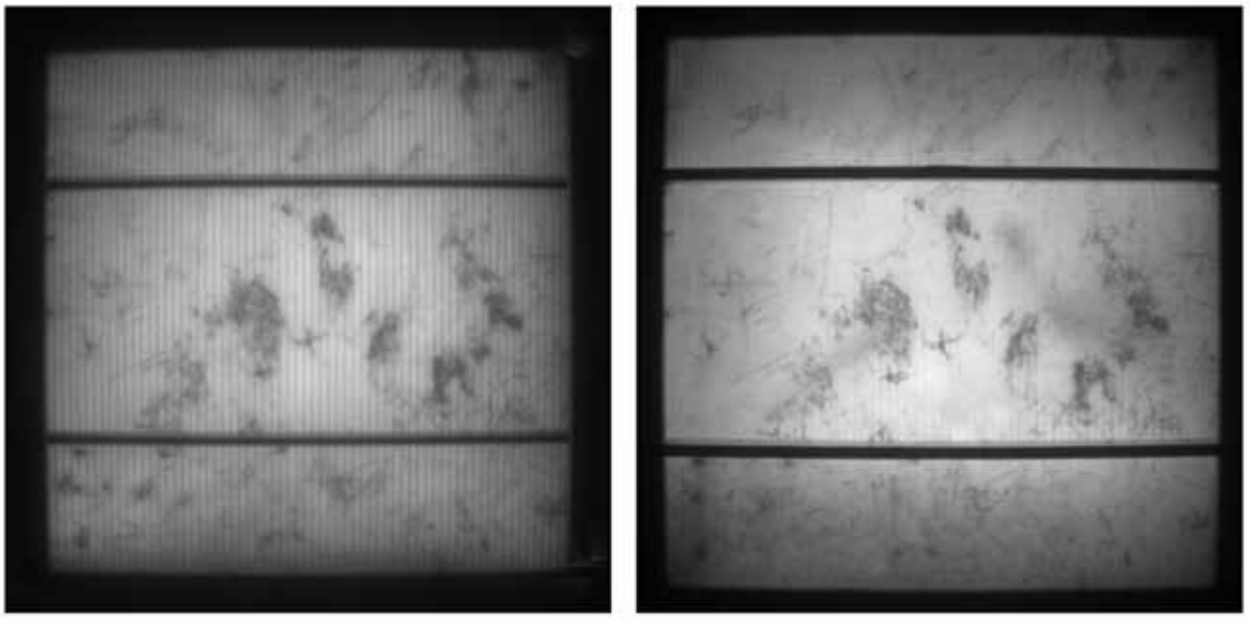

Figure 17. Photoluminescence (left) and electroluminescence (right) maps of a 15.4% efficient 10% UMG solar cell showing high lifetime and good uniformity.

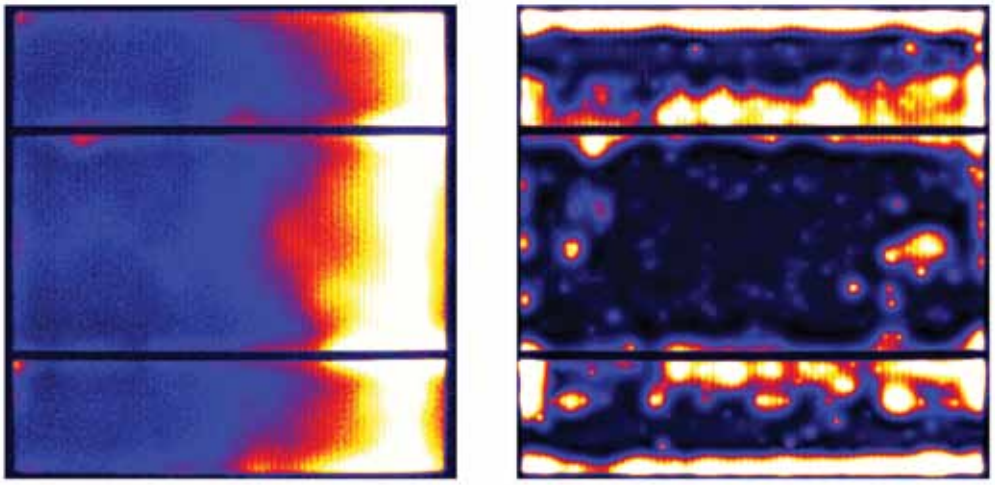

Figure 18. Forward bias (left) and reverse bias (right) DLIT images of the 10% UMG wafer in Figs. 8–11. Excess current is present where light spots appear.

between the low lifetime patches in the LBIC map and low intensity regions in the photoluminescence map.

Similar information can be gained from the electroluminescence map in Fig. 16. Generating such maps requires the application of a forward bias to result in forward bias currents of several amperes. High lifetime regions emit substantial luminescence and appear bright while poor lifetime regions appear dark. Shunted and poor lifetime wafers exhibit dark patches in both photo- and electroluminescence. This device can be contrasted with the luminescence maps of a much better cell shown in Fig. 17, which shows high brightness that is indicative of better minority carrier lifetimes. The uniformity of intensity indicates uniform lifetime and diffusion lengths.

On average, solar cells fabricated from UMG blends and non-UMG (solar-grade) material appear to exhibit the same degree of shunt leakage currents. These probably arise from grain boundaries and dislocation networks resulting from the casting process, which may then be decorated by impurities. The similar short circuit currents and efficiencies of the UMG blends and solar-grade material may be a result of similar background impurity densities as shown in Table 5. For the 100% UMG, the lower lifetimes and photocurrents may be due to higher impurity densities located at these dislocation areas. Iron and copper at were present higher densities in these starting wafers as were boron and phosphorus. Reducing these densities and/or incorporating more aggressive gettering techniques would be beneficial for this material.

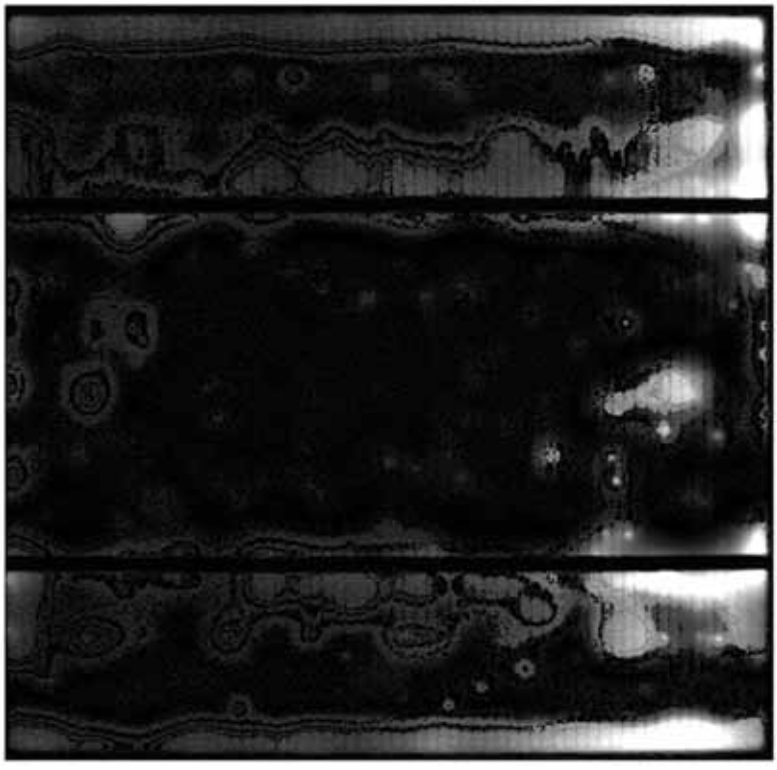

Figure 19. AND image of the forward and reverse DLIT images from Fig. 12 showing ohmic shunts along portions of the busbars and a portion of the edges.

Even in the small sample set available in this series of experiments (15 wafers of each variety), a considerable spread of device performance was observed. Though there were too few wafers to make any statistical conclusions, the shunt leakage was one factor involved in the efficiency variability. The shunts themselves appear to arise when the bus bars and/or fingers cross high dislocation density patches, but a large portion of the wafers also showed strong edge leakage, revealed in DLIT images. These images are made by biasing the cell in either forward or reverse bias and recording hot spots where excess current flows and the temperature rises [5,6]. The temperature is detected by infrared camera and lock-in techniques, resulting in excellent signal-to-noise ratios. Bright (hot) spots may indicate only a few degrees above the surroundings while more serious current channelling may result in spots up to a hundred degrees above. The same spots appearing in both forward and reverse bias are known as ohmic shunts and may be caused by the metal electrode penetrating through the emitter to the base region. Spots appearing in one bias only are diode-like and may be due to several causes [7].

Fig. 18 shows a DLIT image of a 10% UMG cell and indicates the areas where shunts occur (i.e. where excess current is flowing). The probes were uniformly placed along both entire bus bars; therefore the image is caused by a wafer non-uniformity and not the measurement apparatus. In forward bias (left-hand image), current crowding occurs along the right edge and may be due to a lower

sheet resistivity in this region. In reverse bias (right-hand image), many shunts are seen to be covering a significant portion of the cell. Current leakage is prominent along both edges and at various positions along the busbars. Individual shunt areas are also located within the wafer at several individual spots.

By superimposing forward and reverse bias images in logic AND mode, ohmic and diode shunts can be separated. Ohmic shunts appear in both images and therefore in the AND map, while diode shunts disappear. Fig. 19 shows an AND image from the DLIT maps in Fig. 18. Comparing Figs. 18 and 19, only a fraction of the shunt leakages are due to ohmic shunts, where the metal electrodes may penetrate to the base or where doping may be high enough for tunnelling currents to appear. The bulk of the shunts are diode-like and may be associated in some way with grain boundaries or defects at the cell edges.

Summary

This UMG study clearly shows that the use of this material, compared to solar grade, can have significant cost advantages, demonstrated by the economics study comparing both materials. To be competitive, the UMG material must result in similar efficiencies as regular solar grade, i.e., the minority carrier lifetimes must be comparable. Lifetimes in UMG can benefit strongly from gettering, and UMG-based cells processed appropriately result in similar performances compared to solar-grade cells.

Additional follow-on studies would further quantify the potential advantage of UMG material measured in cost/Wp compared to solar-grade material. While manufacturing solar efficiencies are now around 15-16% for the UMG/solar-grade blends, they can be enhanced using selective emitters, improved contacts, and localized back surface fields. The same can be said of solar-grade material, indicating that incremental improvements in a cell manufacturing line does not preclude running UMG, UMG blend, or solar-grade starting materials.

In summary, solar cells made from UMG-based material have the same features as any multicrystalline-based cells except for somewhat higher impurity levels in the 100% UMG. These higher impurities appear to be diluted sufficiently in UMG/solar-grade blends to result in similar efficiencies with the reference solar grade. Quantum efficiencies, short circuit currents and open circuit voltages, and device performance are nearly independent of the UMG blend at least up to 30% UMG. Forensic analysis such as LBIC, photo- and electroluminescence, and DLIT are highly valuable in examining the detailed device behaviour and diagnosing problem areas for future solution. These same techniques are equally valuable in non-UMG solar cells.

Acknowledgment

This material is based upon work supported in part by the US Department of Energy (DOE).

Disclaimer

References

[1] Prettyman, K. & Pfeiffer, G. et al. 2009, "Solar Cell Production using UMG Silicon", *24th EU PVSEC*, Hamburg, Germany.

[2] Bentzen, A. & Holt, A. 2008, "Overview of Phosphorus Diffusion and Gettering in Multicrystalline Silicon", *Materials Science and Eng. B*, doi:10.10.1016 / j.mseb.2008.10.060.

[3] Braga, A.F.B. & Moreira, S.P. et al. 2008, *Solar Energy Materials and Solar Cells*, Vol. 92, p. 418.

[4] Reiman, C. & Jung, T. et al. 2008, *33rd IEEE PVSC*.

[5] Call, N. & Johnston, S. et al. 2009, "Imaging of Shunts and Junction Breakdown in Multicrystalline Si Solar Cells", *34th IEEE PVSC*.

[6] Johnston, S., Call, N. & Ahrenkiel, R. 2009, "Applications of Imaging Techniques for Solar Cell Characterization", *34th IEEE PVSC*.

[7] Kwapil, W., Kasemann, M. et al. 2009, "Physical Mechanisms of Breakdown in Multicrystalline Si Solar Cells", *24th EU PVSEC*, Hamburg, Germany.

[8] Stoddard, N., Wu, B. et al. 2008, *Proc. 18th Workshop on Crystalline Silicon Solar Cells and Modules: Materials and Processes*, NREL/BK-520-45745 (2008).

About the Authors

Rainer Krause has a Ph.D. in electrical engineering and physics. He has worked at IBM in Mainz, Germany for the past 13 years in positions such as engineering manager for automation, test engineering and lithography. He is manager of the ISC (Integrated Supply Chain) technology centre to support IBM WW semiconductor and server activities, and also holds roles such as master inventor, innovation champion and member of the technical expert council and patent review board. He is also a member of the WW solar council within IBM where he coordinates technology-related issues.

Dr. Harold Hovel received his B.S., M.S., and Ph.D. degrees from Carnegie Institute of Technology in 1964, '65, and '68, respectively. He joined the IBM Watson Research Laboratory in 1968 and has been involved in solar cell research for nearly 45 years and authored the first reference book on solar cells, *Solar Cells: Vol. 11 of Semiconductors and Semimetals*, in 1973, and has written many contributed and review papers on various aspects of photovoltaics, including crystalline silicon, gallium arsenide, amorphous Si, heterojunction, multijunctions, organic solar cells and concentrator cells. He is a National Associate of the National Academy of Sciences.

Dr. Eric Marshall performs solar cell research at the IBM TJ Watson Research Center. He received his degrees in applied physics from the University of California–San Diego and has worked as a Research Staff Member at IBM and as Vice President, Strategic Partnerships and Innovation at New York Hall of Science. Topics covered by his publications and presentations (>100) include the correlation of electronic materials and device properties in multicomponent systems. His research applies complementary fabrication and analysis techniques to explore materials and device processing of semiconductor-based systems (IV, III-V, and II-VI).

Gerd Pfeiffer is working in procurement engineering at IBM East Fishkill, NY, and has been involved in PV since 2006. Prior to joining IBM in 2000, he worked as an application engineer at MEMC Electronic Materials. From 1994-98, he was employed by SiBond, L.L.C. in the area of silicon-on-insulator characterization. He received a Ph.D. in physics from North Carolina State University in 1991 and spent three years working as a research associate at the Max-Planck-Institute for Solid State Research in Stuttgart, Germany.

Zhengwen Li has been working for the IBM Semiconductor Research and Development Center for three years, specializing in process development for thin films and metals, using CVD and ALD techniques to make high-dielectrics and metal films for embedded DRAM applications, middle-of-line contact metals, copper interconnect developments, and solar related activities. Zhengwen holds a Ph.D. degree from the chemistry department at Harvard University in 2007, majoring in atomic layer depositions from precursor synthesis and characterizations, to thin-film nucleation and growth.

Dr. Larry Clevenger is a Senior Technical Staff Member at IBM working in the area of Advanced BEOL Integration. He is a noted expert and leader for the innovation, development, and qualification of IBM semiconductor contact and BEOL technologies, and received a B.S. in material engineering from UCLA and a Ph.D. in electronic materials from MIT. He holds 132 issued patents, has co-authored more than 35 technical publications and has two IBM Corporate Technology Awards.

Kevin Petrarca has 19 years' experience in semiconductor development and fabrication through IBM's 200mm Advanced Silicon Technology Center and 300mm fab at the Hudson Valley Research Park in East Fishkill and the IBM T.J. Watson Research Center in NY. Currently working in 3D integration development, he has worked in areas such as manufacturing management, lithography, chemical mechanical polish and materials integration for low-k dielectrics. Kevin has co-authored several technical papers and holds over 60 US patents.

Davood Shahrjerdi joined IBM T. J. Watson Research Center in 2009, where he is currently working on advanced solar cell structures and materials. Davood did his Ph.D. in electrical engineering at The University of Texas at Austin, where he explored various III-V channel materials for CMOS applications. Prior to that, he performed research on self-assembly of nanoparticles for nanocrystal flash memory applications as well as ultra-low temperature crystallization of a-Si and a-Ge for flexible display and sensor applications.

Kevin M. Prettyman has a B.S. in chemistry with minor in physics from Brigham Young University, M.E., a Ph.D. in materials science and engineering from the University of Utah, and an M.B.A. in finance and operations management from New York University's Stern School of Business. A holder of multiple patents, he has managed development groups and manufacturing engineering groups in IBM's multi-layer ceramic and semiconductor areasand drove IBM's efforts in Solid Oxide Fuel Cells, serving as technology leader in photovoltaic devices in various technologies and material sets for IBM's Microelectronic Division.

Dr. Steve Johnston is a research scientist on the Electro-Optical team of the Measurements & Characterization division of NREL. He received his B.S. in engineering from the Colorado School of Mines (CSM); M.S. from the University of Illinois, Urbana-Champaign in electrical engineering; and Ph.D. from CSM in materials science. He has worked for over two years at Texas Instruments and Cray Computers and has over 10 years of experience with NREL in minority-carrier lifetime, capacitance measurements, and most recently, solar cell imaging techniques.

Enquiries

IBM Corporation – Research and
Integrated Supply Chain
Yorktown Heights
NY 10598
USA

Hechtheimerstrasse 2
55131 Mainz
Germany